ENGINEERING TRANSACTIONS • *Enging. Trans.* • 40, 1, 49-62, 1992
Polish Academy of Sciences • Institute of Fundamental Technological Research

MATHEMATICAL MODEL OF AN OVERRUNNING MECHANISM IN A NEW ONE-WAY CLUTCH

S. C. BURGESS, T. A. STOLARSKI and S. KARP (UXBRIDGE)

This paper presents a mathematical model of an overrunning mechanism in a new one-way clutch, called a collapsible-band clutch. The operation of the clutch is explained in general terms, and then the governing equations of the mechanism kinematics are derived. The model is used to calculate critical dimensions in the mechanism and to estimate bending stresses that take place during overrunning.

Notation

- ϕ relative rotation of clutch halves,
- P angular tooth pitch,
- R_I inner radius of teeth of outer clutch half,
- R_0 outer radius of teeth of outer clutch half,
- L angular length of land,
- N number of teeth in outer clutch,
- t depth of tooth,
- m reference point where $\Delta R(m) = t$,
- ΔR radial component of reference point displacement,
- $\Delta\theta$ angular component of reference point displacement,
- R_s radius of spiral curve,
- R_c local radius of curvature of spiral curve,
- δ_s bending stress,
- E elastic modulus of band material,
- y maximum distance from neutral axis.

Remaining symbols are defined where they occur in the text and on the accompanying figures.

1. Introduction

One-way or overrunning clutches transmit torque in one direction of rotation and overrun in the opposite direction. They are used in applications such as drive trains, conveyers and indexing mechanisms. A simple overrunning clutch, called a collapsible-band clutch (Fig.1), was designed at Brunel University in 1985 [1]. The clutch comprises three plastic moulded parts and is suitable for light applications.

In the non-driving direction of rotation, an overrunning clutch disengages the transmission by means of an overrunning mechanism. The overrunning mechanism in the collapsible-band clutch involves the collapsing of a toothed-band. The band is displaced in a complex manner in accordance with the geometrical constraints imposed by the two relatively rotating clutch halves.

The design of the collapsible-band clutch was optimised by developing and using a mathematical model of the mechanism kinematics. This paper describes the overrunning mechanism, derives the equations which model it and gives some examples of results produced from the model.

2. The overrunning mechanism

For overrunning to take place the band has to be displaced from its tooth-engaged position (Fig.1) so that the outer clutch half can rotate relatively anticlockwise to the inner clutch half. In the engaged position the band assumes its free moulded shape, however, its arcuate configuration and the use of thermoplastic material make it resiliently collapsible. This enables

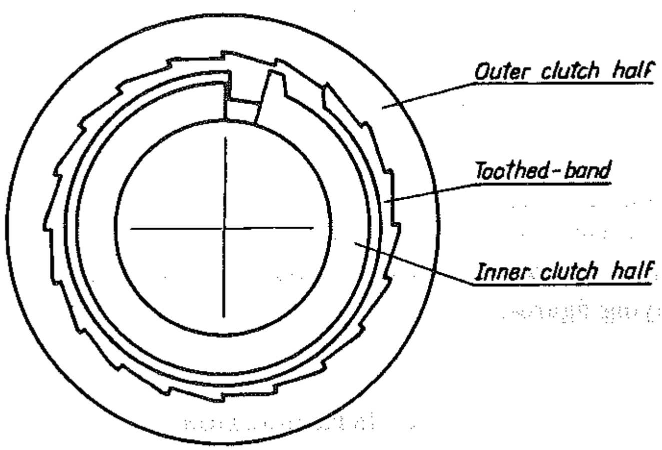

FIG. 1. Collapsible-band clutch.

the teeth of the band to ride under the teeth of the outer clutch half in the non-driving direction of rotation with little frictional torque. Typically, drag is less than 0.5% of drive torque capacity [1].

2.1. The displacement cycle

For each relative rotation of the two clutch halves, ϕ equal to one tooth pitch, P, the band collapses and expands through a radial distance $\Delta R = t$. From Fig.2 it can be seen that the band is not displaced uniformly but that the displacement, $\Delta R = t$ is firstly completed at the front end of the band before propagating anticlockwise to the end of the band. The first tooth is fully deflected as soon as the relative rotation of $\phi = P$ has been achieved (Fig.2b) and this first part of the cycle is termed the collapsing

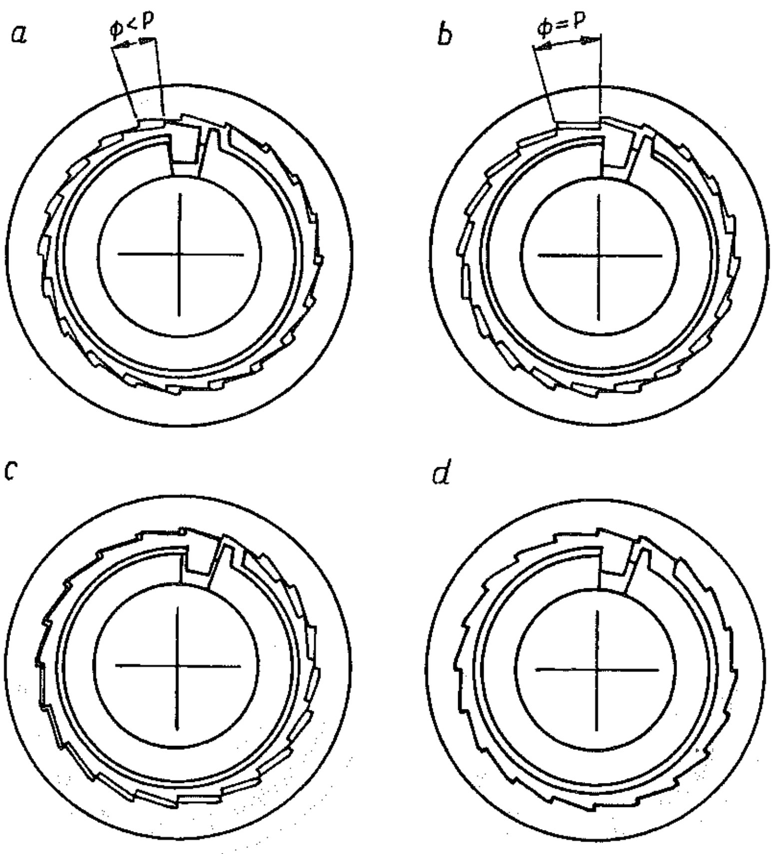

FIG. 2. Progressive stages of the displacement cycle.

phase. After the collapsing phase the displacement, $\Delta R = t$, propagates rapidly through the band without any further relative rotation (Figs.2c and 2d). This happens because once the first tooth has passed under its opposing tooth in the outer clutch half, a vital constraining force is removed and the band releases strain energy, acquired during inward displacement, in snapping back to the position tooth-engagement (Fig.2d). This second part of the displacement cycle is termed the expanding phase.

The complex nature of the band displacements is due to the band having two degrees of freedom. The band is constrained circumferentially at the front end only, therefore when the band is displaced radially inwards, during the collapsing phase and part of the expanding phase, there is also angular displacement in the anticlockwise direction (Figs.2a, 2b and 2c). Likewise, when the band moves radially outwards, during the expanding there is angular displacement in the clockwise direction (Fig.2c). It is necessary to be able to predict the displacements that take place so that the clutch can be designed to have the correct clearances. In particular, there has to be adequate clearance in the slot of the inner clutch half to allow the band enough freedom to expand (Fig.2c). In addition, bending stresses can be estimated from the known displacements.

3. The governing equations of band displacements

The band is modelled by a spiral curve which passes through a set of reference points as shown in Figs.3a and 3b. The reference points are lo-

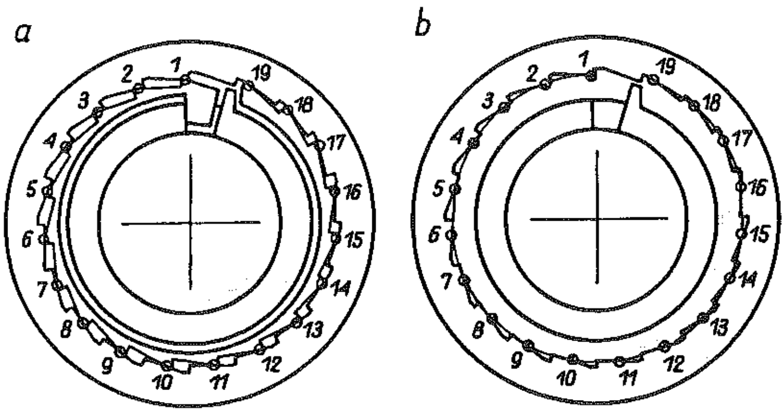

FIG. 3. Displaced band modelled by a single spiral curve.

cated behind each band tooth tip at the back of the land area. This is convenient because the band maintains contact with the inner perimeter of the outer clutch half through the majority of these points during the whole overrunning cycle. Therefore the reference points are boundary points whose co-ordinates can be defined partly by the geometrical profile of the teeth of the outer clutch half.

The instantaneous profile of the displaced band is constructed relative to the spiral curve by assuming that no significant distortion takes place across the section of the band. This assumption is justified due to the slenderness of the band which always has a depth of section much less than 10% of its radius of curvature.

Each reference point has a radial component of displacement, ΔR and an angular component of displacement, $\Delta\theta$ and these relative displacements determine the corresponding new shape of the spiral curve and toothed-band. The radial displacement, ΔR can be defined by the geometry of the instantaneous locus of the spiral curve (Fig.4).

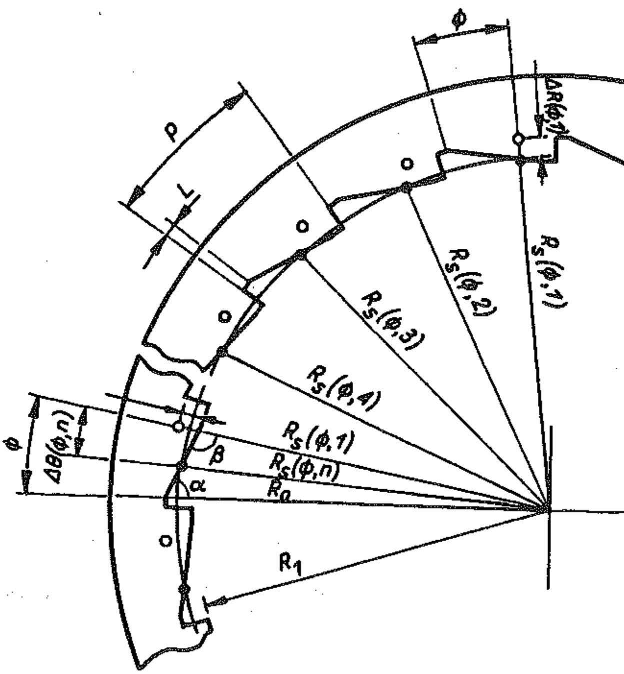

FIG. 4. Instantaneous locus of spiral curve. o undisplaced position of reference point, • displaced position of reference point.

3.1. Radial displacement, ΔR

Because there is no angular displacement at the first tooth, the radius of the spiral curve at the first reference point is only dependent on ϕ:

$$R_s(\phi, 1) = \frac{R_0 \sin(\alpha)}{\sin(\beta)}.$$

Here

$$\begin{aligned}
\alpha &= \sin^{-1}\left(\frac{R_I \sin(P-2L)}{x}\right), \\
x &= \sqrt{R_0^2 + R_I^2 - 2R_0 R_I \cos(P-2L)}\,, \\
\beta &= \pi - \alpha - \phi\,,
\end{aligned}$$

Thus

$$R_s(\phi, 1) = \frac{R_0 R_I \sin(P-2L)}{x \sin(\beta)}\,.$$

The radial displacement of the first reference point is

$$\Delta R(\phi, l) = R_0 - R_s(\phi, 1).$$

Thus

$$\Delta R(\phi, 1) = R_0 \left(\frac{1 - R_I \sin(P-2L)}{x \sin(\beta)}\right). \tag{3.1$_1$}$$

The radial displacements of the remaining reference points which are displaced in the anticlockwise direction (as in Fig.4) are

$$\Delta R(\phi, n) = R_0 - \frac{R_s(\phi, 1)\sin(\beta)}{\sin(\pi - \beta - \Delta\theta(\phi, n))}.$$

Thus

$$\Delta R(\phi, n) = R_0 \left(1 - \frac{R_1 \sin(P-2L)}{x \sin(\pi - \beta - \Delta\theta(\phi, n))}\right). \tag{3.1$_2$}$$

The radial displacements of the remaining reference points which are displaced in the clockwise direction are

$$\Delta R(\phi, n) = R_0 - \frac{R_s(\phi, j)\sin(\pi - \beta)}{\sin(\beta - \Delta\theta(\phi, n))}, \tag{3.1$_3$}$$

where j is the number of the last reference point to be displaced in the clockwise direction.

Because both $\Delta R(\phi, n)$ and $\Delta\theta(\phi, n)$ are unknown in Eqs.$(3.1)_2$ and $(3.1)_3$, it is necessary to define the coordinates of the reference points in a second way. By assuming that the length of the spiral curve remains constant throughout the overrunning cycle, the angular displacement of each point, $\Delta\theta(\phi, n)$, can be equated with the angle of the spiral curve up to that point, $\theta(\phi, n)$, and the average radial displacement up to that point, $\Delta R_{AV}(\phi, n)$. The band can be assumed to remain at a constant length because the forces and direct strains that occur along its length are insignificant.

In order to equate the angular displacement to the average radial displacement, it is necessary to determine the average radius of the spiral curve through sections of its length. This can be done by assuming the spiral curve to have a constant gradient (rate of change of curvature) between individual reference points. This assumption means that the trapezoidal rule of integration will determine the average radius of the spiral curve and the average radial displacement. The assumption is justified because the width of strip between points is relatively small and because the gradient of the spiral is very shallow. In addition, the change of section in the band close to the reference points would tend to create a point of discontinuity at those descrete points.

3.2. Angular displacement $\Delta\theta$

Figure 5 shows the angular displacement $(\tilde{\theta}_n - \theta_n)$ of a circular arc which is displaced radially inwards into a spiral curve of shallow gradient. The angular length of arc $(\tilde{\theta}_n - \theta_n)$ can be defined by equating the separate arc lengths,

$$R_0(\theta_n - \theta_1) = \int_{\theta_1}^{\tilde{\theta}_n} \tilde{R}(\theta) d\theta.$$

Thus

$$R_0(\theta_n - \theta_1) = \int_{\theta_1}^{\theta_n} \tilde{R}(\theta) d\theta - \int_{\theta_n}^{\tilde{\theta}_n} \tilde{R}(\theta) d\theta = 0.$$

The integrals can be replaced by defining the average radius of the spiral

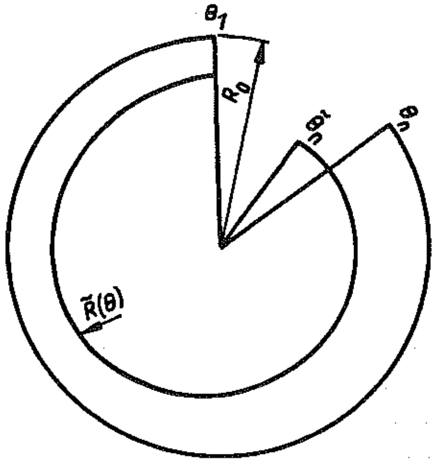

FIG. 5. Local radius of curvature of reference point. ● displaced position of reference point.

curve between $(\theta_n - \theta_1)$ and between $(\tilde{\theta}_n - \theta_n)$:

$$R_{AV} = \frac{\int_{\theta_1}^{\theta_n} \tilde{R}(\theta)d\theta}{(\theta_n - \theta_1)}, \qquad R_1 \approx \frac{\int_{\theta_n}^{\tilde{\theta}_n} \tilde{R}(\theta)d\theta}{(\tilde{\theta}_n - \theta_n)},$$

thus

$$(R_0 - R_{AV})(\theta_n - \theta_1) - R_I(\tilde{\theta}_n - \theta_n) = 0,$$

and

$$(\tilde{\theta}_n - \theta_n) = \frac{(R_0 - R_{AV})(\theta_n - \theta_1)}{R_I}.$$

In the case of the spiral curve passing through n reference points (Fig.3b), the equation can be written in the following way:

$$\Delta\theta(\phi, n) = \frac{\Delta R_{AV}(\phi, n)\theta(\phi, n)}{R_I},$$

where

$$\theta(\phi, n) = \frac{(n-1)2\pi}{N},$$

$$\Delta R(\phi, n)_{AV} = \frac{h}{2}\left\{\Delta R(\phi, 1) + 2\sum_{k=2}^{k=n-1} \Delta R(\phi, k) + \Delta R(\phi, n)\right\},$$

$$h = \frac{1}{n-1}.$$

Thus, the angular displacement of each reference point is

$$\Delta\theta(\phi, n) = \frac{2\pi}{NR_I}\left\{\Delta R(\phi, 1) + 2\sum_{k=2}^{k=n-1}\Delta R(\phi, k) + \Delta R(\phi, n)\right\}. \tag{3.2}$$

4. Solution of equations

4.1. Displacements

The two sets of governing equations for ΔR and $\Delta\theta$ cannot be solved simultaneously by direct substitution because Eqs.$(3.1)_2$ and $(3.1)_3$ are transcendental equations. Therefore the equations are solved by the method of successive substitution. By substituting Eqs.(3.2) into Eqs.$(3.1)_2$, and $(3.1)_3$, implicit equations are formed such that

$$\Delta R(\phi, n) = f\{\Delta R(\phi, n)\}.$$

The equation is solved by successively substituting the answer on the left-hand side of the equation into the right-hand side. By starting with a first approximation of $\Delta R(\phi, n)_1 = 0$ the iterative-substitution procedure typically converges to 0.05% accuracy after five iterations.

For a particular value of ϕ there is a set of $(N-1)$ displacements. It is necessary to solve the governing equations starting at $n = 1$ and progressing up to $n = N - 1$ because the solutions of each reference point requires the solution all preceding points.

The governing equations are solved by a computer program which requests the values of the geometrical variables, R_I, L, N, t and the value or set of values of ϕ. The relative rotation ϕ is an independent variable and determines the instance in the cycle at which the shape of the band is framed. However, when $\phi = P$ the band is in the expanding phase and during this period ϕ is no longer an independent variable. During the expanding phase the tooth number, m, at which the maximum deflection $\Delta R = t$ is occurring, determines the position of the band. Therefore, when $\phi = P, m$ becomes an independent variable and the computer program requests a value or set of values of m between $m = 1$ and $m = N - 1$.

4.2. Bending stresses

The solution of band displacements can be used to estimate the bending stress distribution around the band. By finding the local radius of curvature of the spiral curve at each reference point the bending stress can be estimated in the following way:

$$\sigma_B = Ey\left(\frac{1}{R_c(\phi,n)} - \frac{1}{R_0}\right). \tag{4.1}$$

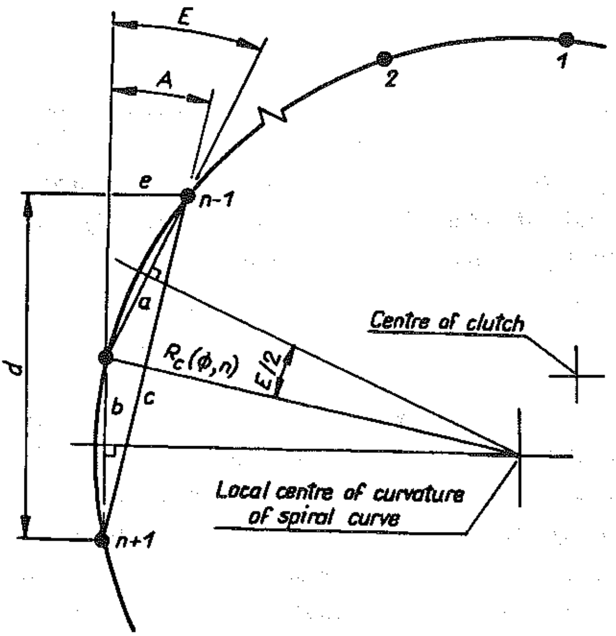

FIG. 6. Circular arc displaced inwards into a spiral curve.

The local radius of curvature of each reference point, $R_c(\phi, n)$ can be estimated by inscribing an arc which passes through the reference point, as well as the preceding and succeeding points (Fig.6):

$$R_c(\phi,n) = \frac{a}{2\sin(E/2)},$$

where a is directly known from the position of reference points, n and $n-1$,

$$E = \tan^{-1}\left(\frac{e}{d-b}\right),$$

b is directly known from the position of reference points, n and $n+1$,

$$d = \frac{b^2 + c^2 - a^2}{2b},$$

c is directly known from the position of reference points, $n-1$ and $n+1$,

$$e = (c^2 - d^2)^{1/2}.$$

The precise value of the bending stress at each point would actually be slightly higher than the mean value obtained in Eq.(4.1) because the change in section of the band behind each tooth would lead to an uneven distribution of stress between points. However, Eq.(4.1) provides an estimate of the stress value and also indicates the nature of stress distribution through the band during the displacement cycle.

5. Results

The computer program which solves the governing equations also contains a graphics plotting program [2] so that results can be studied visually in a convenient way. Figure 2 shows a typical set of results of band displacements. In this example the values of the geometrical variables were: $R_I = 30\,\text{mm}$, $N = 20$, $L = 2$ degrees and $t = 1.1\,\text{mm}$. In addition, the requested value of ϕ were: $\phi(1) = 0.6\,P$ (Fig.2a), $\phi(2) = P$ and $m = 1$ (Fig.2b), $\phi(3) = P$ and $m = 10$ (Fig.2c), and $\phi(4) = P$ and $m = 0$ (Fig.2d). The results in Fig.2 show typical characteristics of band displacements during the displacement cycle. In this example the computer calculated that a clearance of 3 degrees was required in the slot to allow the band to expand. This clearance is an important quantity because the indexing angle of the clutch is equal to the sum of the angular tooth pitch and the slot clearance. The indexing angle, which is the largest possible transfer angle that is required for torque take-up, should preferably be small and comparable with that of a pawl and ratchet clutch. However, it is not necessarily an avantage to have a small tooth pitch because the steeper tooth angle results in higher frictional torque. Therefore, a compromise has to be made between the indexing angle and the frictional torque for each application.

The computer program is also used to plot the results of stress distribution. A typical example of stress distribution during the collapsing phase is shown in Fig.7. The smaller radial displacement of the back of the band at

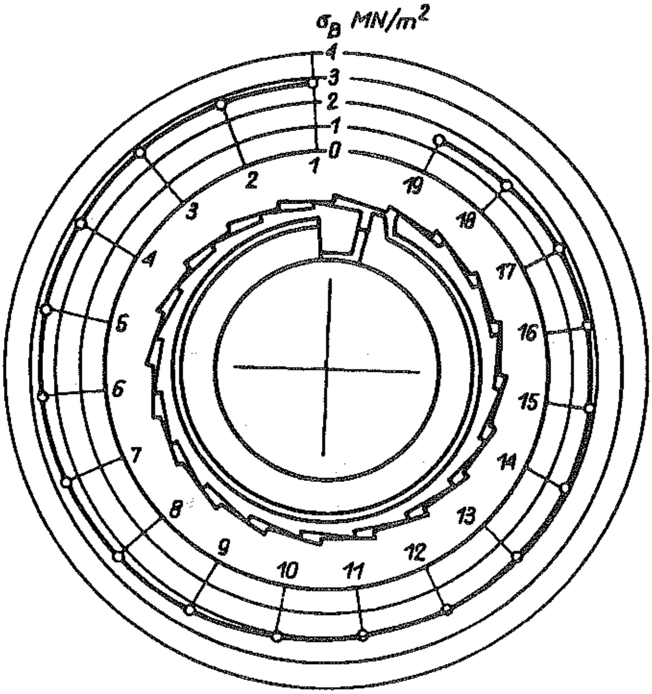

FIG. 7. Stress distribution around band during the collapsing phase.

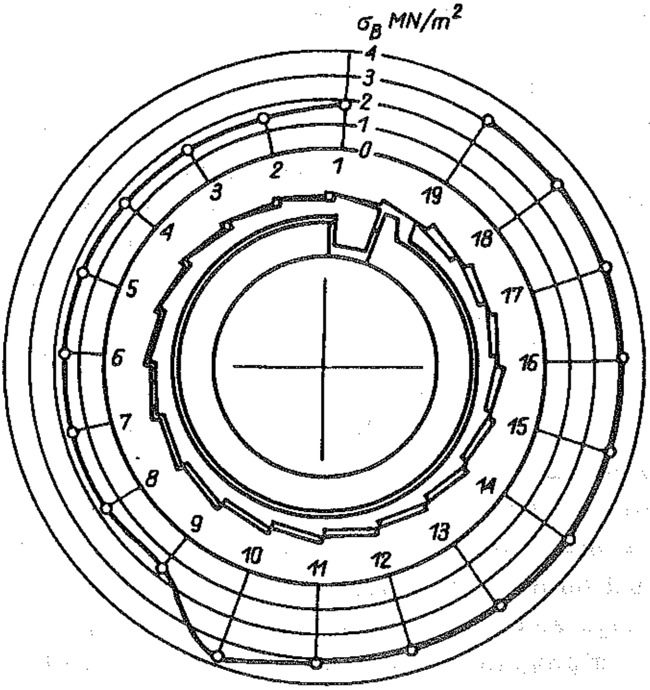

FIG. 8. Stress distribution around band during the expanding phase.

this position results in a gradual decrease in the value of stress from point 1 to 19. A typical example of bending stress distribution during the expanding phase is shown in Fig.8. The main feature in this result is the sudden change in stress that occurs at point number 10. This step in the stress distribution always takes place at the same position of the maximum displacement, $\Delta R(m) = t$. This is because as each band tooth just slides past its corresponding tooth in the outer clutch half, it temporarily loses contact therefore is able to expand outwards suddenly. The maximum displacement propagates through the band rapidly and therefore so does the high stress gradient.

6. Conclusions

The mathematical model has enabled the collapsible-band clutch to be optimised by computer-aided design. Collapsible-band clutches have been manufactured and these have shown that the theoretical predictions of mechanism displacements are correct only for slow overrunning speeds. In practice the band does not continually go through the whole displacement cycle because overrunning speeds are usually too fast for the band to expand during continuous overrunning. The frequency of the displacement cycle is equal to the rotational frequency multiplied by N, the number of teeth. However, the ideal model indicates the maximum displacements that take place.

In tests, polyacetal has been found to be a suitable material for the band, and the use of silicon grease has been found to reduce drag. Within a diameter of 100 mm the collapsible-band can transmit torques up to about 50 Nm. Whilst this is much less than a pawl and ratchet one-way clutch, the collapsible-band clutch has several advantages. The clutch is quieter and lighter and the simple design means that the manufacturing cost for large quantities is very low.

The collapsible-band clutch illustrates how one solid part, made from a thermoplastic material, can be used as a mechanism. In addition, this design exercise shows how the use of computers in the design process can significantly reduce the time and cost of development. The three plastic parts have to be moulded from tool cavities and it would have been very expensive and impractical to manufacture a range of components of different dimensions to study the parameters that affect the performance of the new one-way clutch.

References

1. S.C.Burgess, *Reducing the manufacturing cost of the bicycle freewheel,* Brunel University, 1985.

2. J.Butland, *Simpleplot mark II,* Bradford University Software Services Ltd. (BUSS), 1982.

DEPARTMENT OF MECHANICAL ENGINEERING
BRUNEL UNIVERSITY, UXBRIDGE, MIDDX., UNITED KINGDOM.

Received April 19, 1991.